Carbon Dioxide Fixation by Copper and Silver Halide. Matrix-Isolation FTIR Spectroscopic and DFT Studies of the XMOCO (X = Cl and Br, M = Cu and Ag) Molecules†

Mingfei Zhou,* Luning Zhang, Mohua Chen, Qike Zheng, and Qizong Qin

Laser Chemistry Institute, Fudan University, Shanghai 200433, P. R. China

Received: February 7, 2000; In Final Form: April 27, 2000

The ClCuOCO and BrCuOCO molecules have been observed by cocondensation of the species generated from 1064 nm laser ablation of $CuCl_2$ and $CuBr_2$ targets with CO_2/Ar mixtures. With the aid of density functional calculations and isotopic substituted experiments, infrared absorptions at 2383.9 and 2381.4 cm^{-1} are assigned to the antisymmetric CO_2 stretching vibrations of the ClCuOCO and BrCuOCO molecules in solid argon, respectively. Theoretical calculations predicted these molecules to be linear with a $^1\Sigma^+$ ground state. The interaction between CuX and CO_2 is mainly electrostatic and thus induces a blue shift of the CO_2 antisymmetric stretching vibration. The binding energies for ClCuOCO and BrCuOCO with respect to those for CuX and CO_2 were calculated to be 12.5 and 11.4 kcal/mol, respectively. Similar experiments with AgCl and AgBr gave the analogous ClAgOCO and BrAgOCO. The binding energies were estimated to be 6.5 and 5.9 kcal/mol for ClAgOCO and BrAgOCO, respectively.

Introduction

Conversion of CO_2 into useful chemical materials is an active field in catalytic chemistry[1−3] since carbon dioxide is the most abundant member in the C_1 family. Additionally, carbon dioxide is one of the most important greenhouse gases, and the removal of CO_2 is important from an environmental point of view. Activation of CO_2 by transition metal complexes is believed to be the most promising method for conversion of CO_2 into useful compounds. The interactions between transition metal centers and CO_2 have been intensively studied both experimentally[4−22] and theoretically.[23−28]

Matrix isolation (MI) combined with infrared spectroscopy has been a powerful tool for studying reactions between transition metals and CO_2. Infrared studies suggest that the alkali metal−CO_2 complexes have a rhombic ring structure where the metal atom is interacting equally with both O atoms.[6,7] Spectroscopic studies suggest that silver and gold atoms interact with CO_2 to form weakly bound complexes with side-on structures.[4,5] Mascetti et al. have reported reactions between the first row transition metal atoms and a neat CO_2 matrix.[8,9] Recently, Andrews' group performed a series of studies on the reactions of laser ablated transition metals, including the first row transition metals, Y, Mo, and W, with CO_2.[10−12] Quite recently, studies on the reaction of laser ablated Ta, Nb, and Zr with CO_2 were performed in our group.[13,14]

The interaction between metal cations and CO_2 has also gained extensive attention.[15−22] Theoretical studies predicted that, for the early transition metal cations, the inserted OM^+-CO structure is more stable than that of the linear end-on M^+-OCO isomer, while, for later transition metal cations, the linear end-on M^+OCO structure is the most favorable coordination due to electrostatic interaction.[27,28] The inserted OM^+CO cations (M = Sc, Ti, and V) have been observed in solid argon.[11,12] The binding energies of transition metal cation−CO_2 complexes such as V^+−CO_2, Fe^+−CO_2, Co^+−CO_2, and Ni^+−CO_2 have been measured in the gas phase,[15−18] and different structures have been proposed.

All structurally characterized CO_2 complexes contain transition metal−carbon bonds and possess a bent carbon dioxide ligand.[3] No compounds have yet been isolated in which the CO_2 is bound solely through one oxygen atom, although such species may exist on metal surfaces. In this paper, we report combined matrix-isolation FTIR and DFT studies on the complexes between copper or silver halides (chloride or bromide) and CO_2. Molecules such as XM−OCO (M = Cu and Ag, X = Cl and Br), in which the CO_2 is bound through an O atom, were identified.

Experimental and Theoretical Methods

The experimental setup for pulsed laser ablation and matrix infrared spectroscopic investigation is similar to that described previously.[29,30] The 1064 nm Nd:YAG laser fundamental (Spectra Physics, DCR 2, 20 Hz repetition rate and 8 ns pulse width) was focused onto a rotating metal halide target through a hole in a CsI window. Typically, a 5−10 mJ/pulse laser power was used. The ablated metal halides were codeposited with CO_2 in excess argon onto an 11 K CsI window for 1 h at a rate of 2−4 mmol/h. The CsI window was mounted on a copper holder at the cold end of the cryostat (Air Products Displex DE202) and maintained by a close-cycled helium refrigerator (Air Products Displex IR02W). A Bruker IFS 113v Fourier transform infrared spectrometer equipped with a DTGS detector was used to record the IR spectra in the range 400−4000 cm^{-1}, with a resolution of 0.5 cm^{-1}. Carbon dioxide (Shanghai BOC, 99.99%) and isotopic $^{13}C^{16}O_2$ and $^{12}C^{16}O_2$ + $^{13}C^{16}O_2$ and $^{12}C^{16}O_2$ + $^{12}C^{16}O^{18}O$ + $^{12}C^{18}O_2$ mixtures (Cambridge Isotope Laboratories) were used in different experiments.

Density functional calculations were carried out using the Gaussian 98 program.[31] The three-parameter hybrid functional

† Part of the special issue "C. Bradley Moore Festschrift".

* Corresponding author. E-mail: mfzhou@srcap.stc.sh.cn. Fax: 86-21-65102777.

10.1021/jp000495e CCC: $19.00
Published on Web 07/13/2000

TABLE 1: IR Absorptions (cm^{-1}) from Codeposition of Laser Ablated CuX_2 (X = Cl, Br) Targets with CO_2 in Excess Argon at 11 K

$^{12}C^{16}O_2$	$^{13}C^{16}O_2$	$^{12}C^{16}O_2 + ^{13}C^{16}O_2$	$^{12}C^{16}O_2 + ^{12}C^{16}O^{18}O + ^{12}C^{18}O_2$	assignment
2383.9	2317.4	2384.0, 2317.5	2383.8, 2368.0, 2365.2, 2348.2	ClCuOCO
2381.4				BrCuOCO
2367.9				$ClCu(OCO)_3$
2366.5				$BrCu(OCO)_3$
2356.8	2291.0			$ClCu(OCO)_2$
2356.5				$BrCu(OCO)_2$
2344.9	2279.4	2344.9, 2279.4	2344.8, 2327.6, 2309.7	CO_2
2340.1	2273.6	2339.0, 2273.5	2340.1, 2322.0, 2304.0	CO_2 site
663.5	644.6	663.5, 644.6	663.5, 658.6, 653.6	CO_2
661.9	643.2	661.9, 643.2	661.9, 656.9, 651.9	CO_2 site
513.4	513.4	513.5	513.4	$^{63}Cu^{35}Cl_2$
420.6	420.6	420.6	420.5	$^{63}Cu^{35}Cl$

according to Becke, with additional correlation corrections due to Lee, Yang, and Parr, was utilized (B3LYP).[32,33] Recent calculations have shown that this hybrid functional can provide accurate results for the geometries and vibrational frequencies for transition metal containing compounds.[34,35] The 6-311+G(d) basis sets were used for C, O, Cl, and Br atoms. The basis set of Wachters−Hay, as modified by Gaussian, was used on the Cu atom,[36,37] and the Los Alamos ECP plus DZ (LANL2DZ) was used on the Ag atom.[38] The geometries were fully optimized, and vibrational frequencies were calculated with analytic second derivatives.

Results and Discussion

IR spectra for $CuX_2 + CO_2$ and $AgX + CO_2$ (X = Cl, Br) systems in the Ar matrix will be presented, followed by DFT calculations.

$CuCl_2$, $CuBr_2$ + CO_2/Ar System. Experiments were done using the $CuCl_2$ and $CuBr_2$ targets with different CO_2 concentrations ranging from 0.2% to 0.01%. The absorptions are listed in Table 1. Typical spectra in the antisymmetric CO_2 stretching vibrational region (2300−2400 cm^{-1}) are shown in Figure 1, with 0.03% CO_2 in argon. A 1 h sample deposition at 11 K reveals strong CO_2 absorptions at 2344.9, 2340.1, 663.5, and 661.9 cm^{-1}, sharp sextet absorptions at 513.4, 510.2, 509.3, 506.8, 506.0, and 502.6 cm^{-1}, quartet absorptions at 420.6, 418.2, 413.9, and 411.6 cm^{-1}, and a weak new absorption at 2383.9 cm^{-1}. The CO_2, sextet and quartet absorptions decreased on annealing, while the 2383.9 cm^{-1} absorption greatly increased. Annealing also produced new absorptions at 2356.8 and 2367.9 cm^{-1}. The sextet absorptions exhibit constant relative intensities in all experiments and are due to the antisymmetric stretching vibration of the $CuCl_2$ as a consequence of the Cl and Cu isotope combination. The quartet absorptions showed relative intensities appropriate for CuCl.[39] Experiments with a $CuBr_2$ target resulted in similar spectra. A typical spectrum with 0.1% CO_2 is shown in Figure 1c. Sharp new absorptions at 2381.4, 2366.5, and 2356.5 cm^{-1} appeared after deposition and markedly increased on annealing of the sample to 20−30 K. The $CuBr_2$ and CuBr absorptions were lower than 400 cm^{-1} and were not observed here.

Experiments were done with isotopic-labeled CO_2 samples, and the results are shown in Figures 2 and 3. The 2383.9, 2367.9, and 2356.8 cm^{-1} bands shifted to 2317.4, 2301.7, and 2291.0 cm^{-1} with the $^{13}C^{16}O_2$ sample, and only pure isotopic counterparts were presented for the 2383.9 cm^{-1} band when the mixed $^{12}CO_2 + ^{13}CO_2$ sample was used. In the mixed $C^{16}O_2 + C^{16}O^{18}O + C^{18}O_2$ experiment, a quartet at 2383.8, 2368.0, 2365.2, and 2348.2 cm^{-1} was presented.

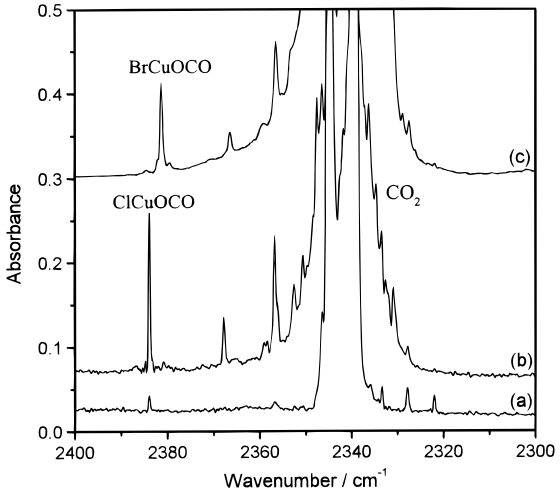

Figure 1. Infrared spectra in the 2400−2300 cm^{-1} region from codeposition of laser ablated copper halides and CO_2 in excess argon: (a) $CuCl_2$ + 0.03% CO_2, 1 h sample deposition at 11 K; (b) after 25 K annealing; (c) $CuBr_2$ + 0.1% CO_2, 1 h sample deposition at 11 K.

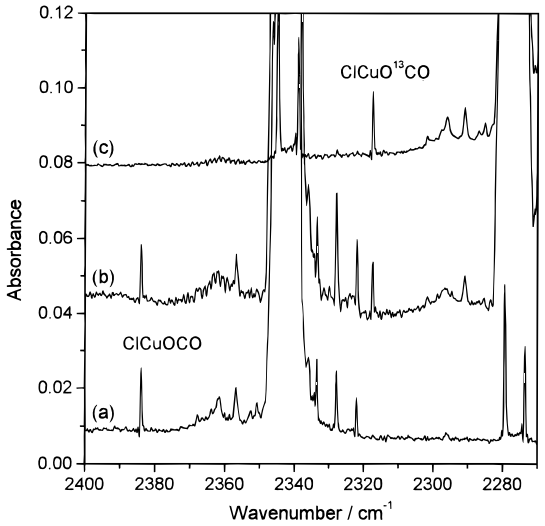

Figure 2. Infrared spectra in the 2400−2270 cm^{-1} region from codeposition of laser ablated $CuCl_2$ and CO_2 in excess argon: (a) 0.03% $^{12}C^{16}O_2$; (b) 0.02% $^{12}C^{16}O_2$ + 0.02% $^{13}C^{16}O_2$; (c) 0.03% $^{13}C^{16}O_2$.

Complementary experiments were done with a $CuCl_2$ target and pure Ar gas. The $CuCl_2$ and CuCl absorptions were observed as before, but no distinctive absorptions were observed in the CO_2 stretching vibrational frequency regions. One experiment was done with a Cu target and 0.5% CO_2 in argon. The CO_2^- absorption at 1657.0 cm^{-1} and the $(CO_2^-)(CO_2)_x$ complex absorption at 1652.8 cm^{-1} were observed,[40] but no absorptions were presented in the high-frequency region of the CO_2 antisymmetric stretching mode.

AgCl, AgBr + CO_2/Ar System. Similar experiments were done with the AgCl and AgBr targets. Figure 4 presents the infrared spectra in the antisymmetric CO_2 stretching vibrational region obtained by codeposition of laser ablated AgX (X = Cl, Br) with CO_2/Ar mixtures at 11 K. The observed band positions are listed in Table 2. As can be seen at 2365.1 and 2355.0 cm^{-1}, new absorptions were observed in the AgCl spectrum (trace

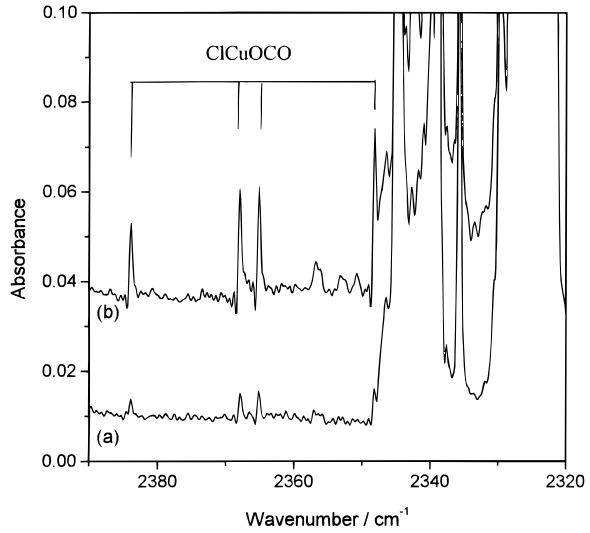

Figure 3. Infrared spectra in the 2390−2320 cm^{-1} region from codeposition of laser ablated $CuCl_2$ and 0.05% ($^{12}C^{16}O_2$ + $^{12}C^{16}O^{18}O$ + $^{12}C^{18}O_2$) in excess argon: (a) 1 h deposition at 11 K; (b) after annealing to 25 K.

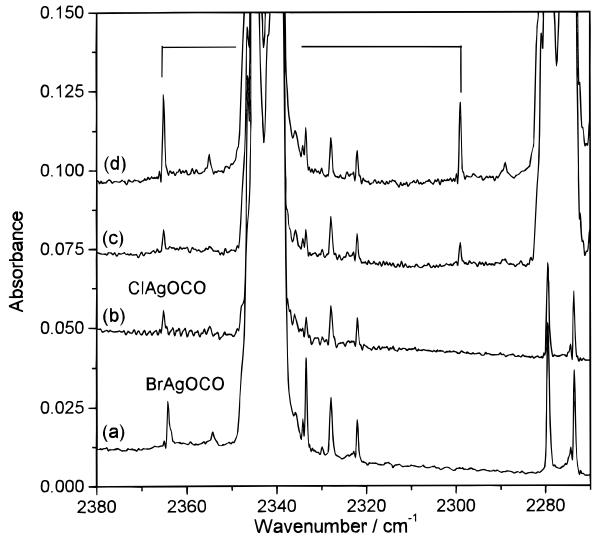

Figure 4. Infrared spectra in the 2380−2270 cm^{-1} region from codeposition of laser ablated silver halides and CO_2 in excess argon: (a) AgBr + 0.03% CO_2, 1 h sample deposition at 11 K; (b) AgCl + 0.03% CO_2, 1 h sample deposition at 11 K; (c) AgCl + 0.02% $^{12}CO_2$ + 0.02% $^{13}C^{16}O_2$, 1 h sample deposition at 11 K; (d) after annealing the sample from part c to 25 K.

TABLE 2: IR Absorptions (cm^{-1}) from Codeposition of Laser Ablated AgX (X = Cl, Br) Targets with CO_2 in Excess Argon at 11K

$^{12}C^{16}O_2$	$^{13}C^{16}O_2$	assignment
2365.1	2299.0	ClAgOCO
2364.2		BrAgOCO
2355.0	2289.0	$ClAg(OCO)_2$
2354.3		$BrAg(OCO)_2$

b). These two bands shifted to 2299.0 and 2289.0 cm^{-1} with the $^{13}C^{16}O_2$ sample, and no obvious intermediate absorptions were observed in the mixed $^{12}CO_2$ + $^{13}CO_2$ experiment (traces c and d). When the AgBr target was used, new absorptions were observed at 2364.2 and 2354.3 cm^{-1} (trace a). These new absorptions were enhanced markedly upon annealing to 20−30 K.

Calculation Results. Calculations were done on different coordination modes of the $XMCO_2$ (M = Cu and Ag, X = Cl and Br) molecules. Only the η^1-O coordination mode with linear structure was converged. Calculations starting from η^1-C coordination converged to MX + CO_2, and the calculations starting from the η^2-C,O side-on structure converged to the linear η^1-O structure. The calculated geometric parameters, the dissociation energies with respect to the ground state MX and CO_2 asymptote, the net metal charge, the Mulliken population, and the vibrational frequencies for the XMOCO molecules are given in Tables 3 and 4, respectively. For comparison, calculation results on the Cu^+OCO and Ag^+OCO cations are also listed.

TABLE 3. Calculated Geometries (Å and deg), Dissociation Energies (kcal/mol), Net Metal Charge, and Mulliken Population Analyses of XMOCO and M^+OCO (M = Cu and Ag, X = Cl and Br)

species	$R_{(XM)}$	$R_{(MO)}$	$R_{(OC)}$	$R_{(CO)}$	D_e[a]	q_M	nd	(n+1)s
ClCuOCO ($^1\Sigma^+$)	2.096	1.989	1.166	1.152	12.5	0.71	9.85	0.42
BrCuOCO ($^1\Sigma^+$)	2.222	2.006	1.166	1.152	11.4	0.67	9.87	0.43
Cu^+OCO ($^1\Sigma^+$)		1.977	1.178	1.141	22.5	0.99	9.96	0.05
ClAgOCO ($^1\Sigma^+$)	2.364	2.377	1.166	1.153	6.5	0.72	9.93	0.34
BrAgOCO ($^1\Sigma^+$)	2.468	2.401	1.166	1.153	5.9	0.68	9.94	0.37
Ag^+OCO ($^1\Sigma^+$)		2.338	1.176	1.145	13.9	1.00	9.99	0.01

[a] Dissociation energies are corrected with zero point energy (ZPE).

ClCuOCO and BrCuOCO. The 2383.9 cm^{-1} band in the $CuCl_2$ + CO_2 reaction was observed on sample deposition and greatly increased on annealing. This band shifted to 2317.4 cm^{-1} with $^{13}C^{16}O_2$ and to 2348.2 cm^{-1} with the $^{12}C^{18}O_2$ sample. The isotopic 12/13 ratio (1.0287) and the isotopic 16/18 ratio (1.0152) indicate that this band is due to an antisymmetric CO_2 stretching vibration. From the doublet feature observed in the mixed $^{12}C^{16}O_2$ + $^{13}C^{16}O_2$ experiment, we can conclude that only one CO_2 unit is involved in this vibrational mode. Of more importance, a quartet with approximately 1:1:1:1 relative intensities was produced in the mixed $^{12}C^{16}O_2$ + $^{12}C^{16}O^{18}O$ + $^{12}C^{18}O_2$ experiment, indicating that two nonequivalent O atoms are involved in this mode. This band is blue-shifted by 39 cm^{-1} from the CO_2 molecule, suggesting that the CO_2 is interacting with a cation via electrostatic interaction. We note that the antisymmetric CO_2 stretching vibrations of CO_2^+ and CO_2^- are observed at 1421 and 1658 cm^{-1} in solid neon.[41] When a $CuBr_2$ target was used, this mode was observed at 2381.4 cm^{-1}, indicating that this mode was slightly coupled with a Cl or Br atom. Accordingly, we assign the absorption at 2383.9 cm^{-1} in the $CuCl_2$ + CO_2 experiment to the antisymmetric CO_2 stretching vibration of the ClCuOCO molecule and the similar absorption at 2381.4 cm^{-1} in $CuBr_2$ + CO_2 experiments to the BrCuOCO molecule.

These assignments receive further support from our DFT calculations. The B3LYP calculations predicted the ClCuOCO molecule to have a linear geometry with a strong antisymmetric CO_2 stretching vibration at 2458.7 cm^{-1}. The antisymmetric CO_2 stretching vibration mode of free CO_2 was predicted to be 2420.8 cm^{-1} at the same level of theory. The predicted 37.9 cm^{-1} blue shift is in good agreement with the experimental observed value of 39.0 cm^{-1}. Of more importance, the calculated isotopic shifts are in excellent agreement with the observed values. As listed in Table 5, the calculation predicted a 69.5 cm^{-1} isotopic shift with $^{13}C^{16}O_2$, and experimental observation gave a 66.5 cm^{-1} shift. In the mixed $^{12}C^{16}O_2$ + $^{12}C^{16}O^{18}O$ + $^{12}C^{18}O_2$ experiment, the calculation predicted a quartet with 17.0/2.8/18.0 cm^{-1} band separations, and we observed 15.8/2.9/17.0 cm^{-1} separations. For BrCuOCO, the observed antisymmetric CO_2 vibration is 36.5 cm^{-1} blue-shifted from that of the free CO_2 (2344.9 cm^{-1}) and is observed at 2381.4 cm^{-1}. This mode was predicted to be 2456.4 cm^{-1}. The calculated 35.6 cm^{-1} shift is also very close to the observed value. From ClCuOCO

TABLE 4. Calculated Vibrational Frequencies (cm^{-1}) and Intensities (kcal/mol) of XMOCO and M^+OCO (M = Cu and Ag, X = Cl and Br)

Cu^+OCO	ClCuOCO	BrCuOCO	Ag^+OCO	ClAgOCO	BrAgOCO
2468.0(861) (σ)	2458.7(1042) (σ)	2456.4(1087)	2451.0(833) (σ)	2442.7(992) (σ)	2440.8(1034)
1393.0(38) (σ)	1391.5(0.3) (σ)	1389.9(0.6)	1383.1(34) (σ)	1385.9(7) (σ)	1384.9(7)
628.7(76) (π)	629.2(68) (π)	630.5(68)	646.1(76) (π)	652.5(70) (π)	653.4(68)
249.9(13) (σ)	413.3(33) (σ)	327.0(21)	167.8(11) (σ)	314.5(31) (σ)	238.6(19)
33.8(4) (π)	200.6(0.1) (σ)	172.9(0.2)	83.7(2) (π)	129.1(1) (σ)	116.9(1)
	108.2(4) (π)	92.5(2)		89.8(4) (π)	83.3(1)
	19.7i(6) (π)	17.2i(2)		25.2(8) (π)	11.2(4)

TABLE 5. Calculated and Observed Isotopic Shifts for ClMOCO (M = Cu and Ag) Relative to $ClM^{16}O^{12}C^{16}O$

	ClCuOCO		ClAgOCO	
	calcd	exptl	calcd	exptl
$^{13}C^{16}O_2$	69.8	66.5	69.6	66.1
$^{18}OC^{16}O$	17.0	15.8		
$^{16}OC^{18}O$	19.8	18.7		
$^{18}OC^{18}O$	37.8	35.7		

to BrCuOCO, we note that the relative band positions have only about a 2.5 cm^{-1} difference. This difference was predicted to be 2.3 cm^{-1} at the B3LYP/6-311+G(d) level.

As listed in Table 4, the OCO symmetric stretching, OCO bending, and X−Cu and Cu−O stretching vibrations were predicted to be much weaker than the antisymmetric CO_2 stretching vibration and, therefore, were not observed here. It should also be noted that there is one imaginary vibrational frequency (−19.7 cm^{-1}) for linear ClCuOCO and BrCuOCO molecules. Optimizations without symmetry constraint, starting with bent geometries, result in a nearly linear structure of ClCuOCO. It has almost the same electronic energy as that of the linear structure and also possesses an imaginary frequency (−18.8 cm^{-1}). When the convergence criteria were increased, the imaginary frequency decreased to −7.6 cm^{-1}. This indicates that the imaginary frequency might be caused by a numerical noise problem. Thus, we believe that ClCuOCO and BrCuOCO molecules should have linear structures.

ClAgOCO and BrAgOCO. Similar bands at 2355.0 and 2354.3 cm^{-1} were observed in the AgCl + CO_2 and AgBr + CO_2 experiments and are assigned to the antisymmetric CO_2 stretching vibrations of the ClAgOCO and BrAgOCO molecules, following the examples of the ClCuOCO and BrCuOCO molecules. Present DFT calculations predicted the ClAgOCO and BrAgOCO molecules to have linear geometry with $^1\Sigma^+$ ground states. The antisymmetric CO_2 stretching vibrations were calculated to be 2442.7 and 2440.8 cm^{-1}, respectively, which must be scaled by 0.964 and 0.965 to match the observed values. Note the scale factor for the CO_2 is 0.969.

Other Absorptions. The 2356.8 and 2367.9 cm^{-1} bands in the $CuCl_2$ + CO_2 experiments were present after sample deposition in high CO_2 concentration experiments, but in lower concentration experiments, these two bands only appeared on annealing. Both bands showed typical antisymmetric CO_2 stretching vibrational frequency ratios, but the mixed isotopic structures could not be resolved due to overlap with the strong CO_2 absorptions and isotopic dilutions. These two bands increased greatly on annealing after the ClCuOCO absorption. The 2356.8 cm^{-1} band appeared earlier than the 2367.9 cm^{-1} band and is tentatively assigned to the antisymmetric CO_2 stretching vibration of the $ClCu(OCO)_2$ molecule, while the 2367.9 cm^{-1} band is tentatively assigned to the $ClCu(OCO)_3$ molecule. Similar bands at 2356.5 and 2366.5 cm^{-1} in the $CuBr_2$ + CO_2 experiments are tentatively assigned to the $BrCu(OCO)_2$ and $BrCu(OCO)_3$ molecules. The 2355.0 cm^{-1} band in the AgCl + CO_2 experiment and the 2354.0 cm^{-1} band in the AgBr + CO_2 experiment are tentatively assigned to the $ClAg(OCO)_2$ and $BrAg(OCO)_2$ molecules, respectively, for the same reason.

Reaction Mechanism and Bonding

The XMOCO molecules are formed by reactions between MX and CO_2, reactions 1−4, which were calculated to be exothermic. The XMOCO absorptions increased markedly on annealing, suggesting that these reactions require no activation energy.

$$CuCl + CO_2 \rightarrow ClCuOCO \qquad \Delta E = -12.5 \text{ kcal/mol} \quad (1)$$

$$CuBr + CO_2 \rightarrow BrCuOCO \qquad \Delta E = -11.4 \text{ kcal/mol} \quad (2)$$

$$AgCl + CO_2 \rightarrow ClAgOCO \qquad \Delta E = -6.5 \text{ kcal/mol} \quad (3)$$

$$AgBr + CO_2 \rightarrow BrAgOCO \qquad \Delta E = -5.9 \text{ kcal/mol} \quad (4)$$

Mascetti and co-workers have studied the Cu−CO_2 complex in the CO_2 matrix, and they suggested a side-on or end-on coordination complex.[8] Hartree−Fock CI [HF(CI)] calculations by Barthelat et al.[23] suggest that only the end-on complex seems to be consistent with the infrared spectra observed in the CO_2 matrix.[23] HF(CI) calculations predicted the CO_2 unit in CuOCO to be almost the same as CO_2^-, with an OCO angle of 135.0°. However, at our B3LYP/6-311+G(d) level of theory, the η^1-O end-on coordinated Cu−CO_2 was found to be a weakly bound van der Waals complex with a Cu−O bond of 4.62 Å and a nearly linear CO_2 moiety. This is quite different from HF(CI) results. However, we also noticed that the bonding mode in ClCuOCO is quite different from the end-on CuOCO mode. The interaction between CuCl and CO_2 is much stronger, and the Cu−O distance is calculated to be 1.989 Å, which is 2.6 Å shorter than that in CuOCO. Ozin et al.[4] have studied the interaction of CO_2 with Ag atoms, and infrared, Raman, and UV−vis spectroscopy suggest a weakly bound side-on Ag−CO_2 complex with a near linear CO_2 unit.

The coordination between CO_2 and transition metal complexes has been the subject of intensive theoretical studies.[25,42] CO_2 interacting with metal complexes can have four coordination modes, namely the η^1-C mode, the η^2-C,O side-on mode, the η^2-O,O mode, and the η^1-O end-on mode. Spectroscopic studies indicated that the bonding on alkali metal−CO_2 complexes is mainly ionic and that the η^2-O,O coordination is favored. However, all structurally characterized transition metal−CO_2 complexes preferred either the η^1-C coordination mode or the η^2-C,O side-on coordination mode.[3] No compounds have yet been isolated in which the linear CO_2 is bound solely through one O atom, although such species may exist on metal surfaces. The presently characterized XCuOCO and XAgOCO provide a good example of a transition metal−CO_2 complex

that has an η^1-O end-on coordination mode, and we believe the CO_2 coordination mode observed in the present study is unique.

As can be seen in Table 3, the net charges on copper and silver atoms in XCuOCO and XAgOCO are about +0.7. The XCuOCO and XAgOCO molecules can be viewed as X^-Cu^+OCO and X^-Ag^+OCO, so the bonding between XM and OCO is quite similar to that of M^+OCO, which is mainly electrostatic. The interaction between transition metal cations and CO_2 has been experimentally studied in the gas phase, and the binding energies have been measured.[15−20] The geometry of the Co^+OCO was found to be linear from the rotational spectrum.[18] By comparing the experimental binding energies of Ni^+CO_2 and Ni^+N_2O, Ni^+CO_2 was suggested to have a T-shaped structure with η^1-C coordination,[15,43] but theoretical calculations indicated that the most stable Ni^+CO_2 isomer has a linear structure.[27,28,44] Present DFT calculations predicted that the T-shaped Cu^+CO_2 and Ag^+CO_2 cation isomers were higher in energy than the linear Cu^+OCO and Ag^+OCO cations. The results on Cu^+OCO are in good agreement with recently reported ab initio and DFT calculations.[27,28] As there are no spectroscopic data on Cu^+OCO and Ag^+OCO, the XCuOCO and XAgOCO molecules observed here can provide some information to estimate the properties of the M^+OCO cations. As can be seen in Tables 3 and 4, the electrostatic interaction causes asymmetry in the two CO bond lengths. In the XCuOCO and XAgOCO molecules, the CO bond length adjacent to the metal increases about 0.005 Å, while the other CO bond length decreases about 0.008 Å when compared to that of the free CO_2 molecule. The variation of the CO_2 geometry in Cu^+OCO and Ag^+OCO is slightly more than that in XMOCO. The metal−O distance in XMOCO is slightly longer than that of the M^+OCO cations. But the Ag−O distance is much greater than the Cu−O distance due to the larger radial extent of the Ag^+ ion. The antisymmetric CO_2 stretching vibrations of Cu^+OCO and Ag^+-OCO were predicted to be 9.3 and 8.3 cm^{-1} higher than those of the ClCuOCO and ClAgOCO molecules. Accordingly, the antisymmetric CO_2 stretching vibrations of Cu^+OCO and Ag^+-OCO should be observed at around 2393 and 2373 cm^{-1} in solid argon.

The dissociation energies of XMOCO with respect to MX + CO_2 are listed in Table 3. The dissociation energies of ClMOCO and BrMOCO are very close, with that for ClMOCO being slightly higher. XMOCO is more weakly bound than the M^+-OCO cations, and the dissociation energies of XMOCO are only about half those of the M^+OCO cations. Comparing Cu with Ag, the binding energies of XAgOCO molecules are lower than those of the XCuOCO molecule.

The bonding mechanism of transition metal−CO_2 complexes has been discussed previously.[23−25,42] In the η^1-O coordination mode, repulsive interactions occur between the doubly occupied dπ orbital and the π orbitals of CO_2, and/or between an occupied σ typical orbital and a σ lone pair orbital on the oxygen atom of CO_2. The metal−OCO repulsion can be reduced by s to d promotion or sdσ hybridization. For Cu^+ and Ag^+, the first excited $d^9s^1(^1D)$ state lies at about 75 and 131 kcal/mol, respectively, above the ground state,[45] so sdσ hybridization is energetically unfavorable. As can be seen in Table 3, there is a larger s population and a smaller d population of XMOCO compared with M^+OCO, indicating less sdσ hybridization and more σ repulsion. Thus, the dissociation energies of XMOCO are smaller than that of the M^+OCO cations.

Conclusions

Laser ablated copper and silver halides reacted with CO_2 molecules to give the XMOCO molecules (X = Cl and Br, M = Cu and Ag), which have been isolated in solid argon. Density functional calculations indicated that these molecules are linear with the CO_2 bound solely through one oxygen atom. The interaction between MX and CO_2 is mainly electrostatic and thus induces a blue shift of the CO_2 antisymmetric stretching vibration. The binding energies for ClCuOCO, BrCuOCO, ClAgOCO, and BrAgOCO with respect to MX and CO_2 were calculated to be 12.5, 11.4, 6.5, and 5.9 kcal/mol, respectively.

The excellent agreement with frequencies and isotopic frequency shifts from density functional calculations strongly supports the vibrational assignments and the identification of these transition metal complexes.

Acknowledgment. This work was supported by the NK-BRSF project of China.

References and Notes

(1) Braunstein, P.; Matt, D.; Nobel, D. *Chem. Rev.* **1988**, *88*, 747.
(2) Cutler, A. R.; Hanna, P. K.; Vites, J. C. *Chem. Rev.* **1988**, *88*, 1363.
(3) Gibson, D. H. *Chem. Rev.* **1996**, *96*, 2063.
(4) Ozin, G. A.; Huber, H.; McIntosh, D. *Inorg. Chem.* **1978**, *17*, 1472.
(5) Huber, H. *Inorg. Chem.* **1977**, *16*, 975.
(6) Jacox, M. E.; Milligan, D. E. *Chem. Phys. Lett.* **1974**, *28*, 163.
(7) Kafafi, Z. H.; Hauge, R. H.; Billups, W. E.; Margrave, J. L. *J. Am. Chem. Soc.* **1983**, *105*, 3886; *Inorg. Chem.* **1984**, *23*, 177.
(8) Mascetti, J.; Tranquille, M. *J. Phys. Chem.* **1988**, *92*, 2177.
(9) Galan, F.; Fouassier, M.; Tranquille, M.; Mascetti, J. *J. Phys. Chem. A* **1997**, *101*, 2626.
(10) Souter, P. F.; Andrews, L. *J. Am. Chem. Soc.* **1997**, *119*, 7350.
(11) Zhou, M. F.; Andrews, L. *J. Am. Chem. Soc.* **1998**, *120*, 13230.
(12) Zhou, M. F.; Andrews, L. *J. Phys. Chem. A* **1999**, *103*, 2013, 2066.
(13) Wang, X. F.; Chen, M. H.; Zhang, L. N.; Qin, Q. Z. *J. Phys. Chem. A* **2000**, *104*, 758.
(14) Zhang, L. N.; Wang, X. F.; Chen, M. H.; Qin, Q. Z. *Chem. Phys.* **2000**, *254*, 231.
(15) Asher, R. L.; Bellert, D.; Buthelezi, T.; Brucat, P. J. *Chem. Phys. Lett.* **1995**, *243*, 269.
(16) Schwartz, J.; Schwartz, H. *Organometallics* **1994**, *13*, 1518.
(17) Lesson, D. E.; Asher, R. L.; Brucat, P. J. *J. Chem. Phys.* **1991**, *95*, 1414.
(18) Asher, R. L.; Bellert, D.; Buthelezi, T.; Brucat, P. J. *Chem. Phys. Lett.* **1994**, *227*, 623.
(19) Sievers, M. R.; Armentrout, P. B. *J. Chem. Phys. A* **1998**, *102*, 10754.
(20) Sievers, M. R.; Armentrout, P. B. *Inorg. Chem.* **1999**, *38*, 397.
(21) Yeh, C. S.; Willey, K. F.; Robbins, D. L.; Pilgrim, J. S.; Duncan, M. A. *J. Chem. Phys.* **1993**, *98*, 1867.
(22) Brock, L. R.; Duncan, M. A. *J. Phys. Chem.* **1995**, *99*, 16571.
(23) Caballol, R.; Marcos, E. S.; Barthelat, J. C. *J. Phys. Chem.* **1987**, *91*, 1328.
(24) Sirois, S.; Castro, M.; Salahub, D. R. *Int. J. Quantum Chem.* **1994**, *28*, 645.
(25) Dedieu, A.; Bo, C.; Ingold, F. In *Metal−Ligand Interactions: From Atoms, to Clusters, to Surfaces;* Salahub, D. R., Russo, N., Eds.; Kluwer Academic Publishers: Norwell, MA, 1992.
(26) Papai, I.; Mascetti, J.; Fournier, R. *J. Phys.Chem. A* **1997**, *101*, 4465.
(27) Sodupe, M.; Branchadell, R. M.; Bauschlicher, C. W., Jr. *J. Phys. Chem. A* **1997**, *101*, 7854.
(28) Fan, H. J.; Liu, C. W. *Chem. Phys. Lett.* **1999**, *300*, 351.
(29) Chen, M. F.; Wang, X. F.; Zhang, L. N.; Yu, M.; Qin, Q. Z. *Chem. Phys.* **1999**, *242*, 81.
(30) Burkholder, T. R.; Andrews, L. *J. Chem. Phys.* **1991**, *95*, 8697.
(31) Frisch, M. J.; Trucks, G. W.; Schlegel, H. B.; Scuseria, G. E.; Robb, M. A.; Cheeseman, J. R.; Zakrzewski, V. G.; Montgomery, J. A., Jr.; Stratmann, R. E.; Burant, J. C.; Dapprich, S.; Millam, J. M.; Daniels, A. D.; Kudin, K. N.; Strain, M. C.; Farkas, O.; Tomasi, J.; Barone, V.; Cossi, M.; Cammi, R.; Mennucci, B.; Pomelli, C.; Adamo, C.; Clifford, S.; Ochterski, J.; Petersson, G. A.; Ayala, P. Y.; Cui, Q.; Morokuma, K.; Malick, D. K.; Rabuck, A. D.; Raghavachari, K.; Foresman, J. B.; Cioslowski, J.; Ortiz, J. V.; Baboul, A. G.; Stefanov, B. B.; Liu, G.; Liashenko, A.; Piskorz, P.; Komaromi, I.; Gomperts, R.; Martin, R. L.; Fox, D. J.; Keith, T.; Al-Laham, M. A.; Peng, C. Y.; Nanayakkara, A.; Gonzalez, C.; Challacombe, M.; Gill, P. M. W.; Johnson, B.; Chen, W.; Wong, M. W.; Andres, J. L.; Gonzalez, C.; Head-Gordon, M.; Replogle, E. S.; Pople, J. A. *Gaussian 98*, Revision A.7; Gaussian, Inc.: Pittsburgh, PA, 1998.
(32) Becke, A. D. *J. Chem. Phys.* **1993**, *98*, 5648.
(33) Lee, C.; Yang, E.; Parr, R. G. *Phys. Rev. B* **1988**, *37*, 785.

(34) Bauschlicher, C. W., Jr.; Ricca, A.; Partridge, H.; Langhoff, S. R. In *Recent Advances in Density Functional Theory*; Chong, D. P., Ed.; World Scientific Publishing: Singapore, 1997; Part II.

(35) Bytheway, I.; Wong, M. W. *Chem. Phys. Lett.* **1998**, *282*, 219.

(36) McLean, A. D.; Chandler, G. S. *J. Chem. Phys.* **1980**, *72*, 5639. Krishnan, R.; Binkley, J. S.; Seeger, R.; Pople, J. A. *J. Chem. Phys.* **1980**, *72*, 650.

(37) Wachter, J. H. *J. Chem. Phys.* **1970**, *52*, 1033. Hay, P. J. *J. Chem. Phys.* **1977**, *66*, 4377.

(38) Hay, P. J.; Wadt, W. R. *J. Chem. Phys.* **1985**, *82*, 299.

(39) Nakamoto, N. *Infrared and Raman Spectra of Inorganic and Coordination Compounds*, 1977.

(40) Zhou, M. F.; Andrews, L. *J. Chem. Phys.* **1999**, *110*, 2414.

(41) Jacox, M. E.; Thompson, W. E. *J. Chem. Phys.* **1989**, *91*, 1410.

(42) See, for example: Sakaki, S.; Kitaura, K.; Morokuma, K. *Inorg. Chem.* **1982**, *21*, 760. Sakaki, S.; Kitaura, K.; Morokuma, K.; Ohkubo, K. *Inorg. Chem.* **1983**, *22*, 104.

(43) Bellert, D.; Buthelezi, T.; Lewis, V.; Dezfulian, K.; Brucat, P. J. *Chem. Phys. Lett.* **1995**, *240*, 495.

(44) Heinemann, C.; Schwarz, J.; Schwarz, H. *Chem. Phys. Lett.* **1995**, *247*, 611.

(45) Moore, C. E. *Atomic Energy Levels*; National Bureau of Standards, U.S. GPO: Washington, DC, 1949.